

Received 9 November 2023, accepted 26 November 2023, date of publication 30 November 2023,  
date of current version 6 December 2023.

Digital Object Identifier 10.1109/ACCESS.2023.3338373

## APPLIED RESEARCH

# Development of Wireless Smart Sleeve Using Pressure Sensitive Resistor

KRANTHI KUMAR PULLURI<sup>1</sup>, VAEGAE NAVEEN KUMAR<sup>1</sup>, (Senior Member, IEEE),  
KALAPRAVEEN BAGADI<sup>2</sup>, (Member, IEEE), VISALAKSHI ANNEPU<sup>3</sup>,  
AND FRANCESCO BENEDETTO<sup>4</sup>, (Senior Member, IEEE)

<sup>1</sup>School of Electronics Engineering, Vellore Institute of Technology, Vellore 632014, India

<sup>2</sup>School of Electronics Engineering, VIT-AP University, Amaravati 522237, India

<sup>3</sup>School of Computer Science and Engineering, VIT-AP University, Amaravati 522237, India

<sup>4</sup>Signal Processing for Telecommunications and Economics Laboratory, Economics Department, University of Roma Tre, 00146 Rome, Italy

Corresponding authors: Francesco Benedetto (francesco.benedetto@uniroma3.it) and Kalapraveen Bagadi (kpbagadi@gmail.com)

**ABSTRACT** Tactile pressure sensors have gained ever increasing attention in designing flexible electronics, such as wearable devices. Building a pressure sensor characterized by high sensitivity and low implementation costs is a very critical challenge to satisfy. Recently, a new low-cost pressure sensor, namely Velostat, has been proposed. Due to its properties of changing its resistance with either flexing or pressure, it has become popular for making inexpensive sensors for microcontroller experiments. Here, we design a smart sleeve made of Velostat to perform rudimentary controls on a smartphone. We first evaluate the optimum layout of the sensor by conducting three tests on the sensor property, such as area of contact, Velostat area, and layers of Velostat. Based on the test performance, a sensor patch is designed. Then, we develop a novel resistive signal conditioning circuit to convert the pressure on the sensor patch into an electrical signal to be transmitted to smartphones via Bluetooth. Finally, we have also realized an Android application that performs the required operations (e.g., multimedia player controller and an SOS alert system) on the smartphone based on the received sensor data. The functionality of our smart sleeve system is validated in real-time, showing promising results for the design of low-cost smart wearables.

**INDEX TERMS** Bluetooth low energy, resistive signal conditioning, smart wearable, tactile pressure sensors, velostat.

## I. INTRODUCTION

The demand for the ability to perform trivial tasks quickly on the go is ever-growing with the increase in the pace of today's lifestyle [1]. Sensors have significantly contributed to making life easier in numerous ways across various fields and industries [2], [3]. Basic smartphone operations tend to have long and overly complicated operational procedures [4]. They also inevitably require the user to hold the phone to perform the required tasks. It may not be feasible every time. Hence, a sensor embedded and readily available in the sleeve of clothing apparel makes it highly functional and easy to perform tasks. Pressure sensors have been else developed to convert pressure information into electrical

signals. In particular, piezoresistive [5], capacitive [6], piezoelectric [7], and triboelectric [8] sensors have been studied in the literature with different performances. The piezoresistive pressure sensors have demonstrated to be the best choice for the design of wearable next-generation flexible pressure sensors due to their great sensitivity, ease structure, fast response, low cost, and robust anti-interference capability [9]. Chen et al. [10], proposed a soaking approach to fabricate porous sponge pressure sensors. The structure exhibits high sensitivity, a wide pressure detection range, quick response/release time, and good reproducibility. Zhang et al. [11], developed a smart glove that exploits pressure sensors composed of mesh-like micro-convex structure polydimethylsiloxane (PDMS), MXene nanosheet/Ag nanoflower (AgNF) films, and flexible interdigital electrodes was designed by layer-by-layer (LBL) assembly. Xia et al. [12] implemented a

The associate editor coordinating the review of this manuscript and approving it for publication was Alon Kuperman<sup>1</sup>.

flexible pressure sensor based on Layer-by-layer (LbL) self-assembly of the MXene/carbon black (CB) on a polyurethane (PU) sponge is reported. The sensor has shown excellent performance in controlling smart devices through external pressure as a human-machine interface. Then, in [13], a conductive and biocompatible hybrid hydrogel was assembled into an adhesive, flexible wearable sensor for ultrasensitive human-computer interaction and smart detection. The Velostat piezoresistive material, also known as Linqstat, was developed by Custom Materials, now part of the 3M company, and was later purchased by “Desco Industries” in 2015, becoming a US brand [14]. It is a packaging material constituted by a polymeric layer (polyolefins) impregnated with carbon powder to make it electrically conductive. Its main feature is to change its electric resistance with bending or pressure due to the changing of the geometric parameters (see Fig. 1). Since the layer’s resistance decreases when pressure is applied, this reading can indicate when the weight is applied or removed from the sensor.

Velostat is characterized by the following parameters [15]: (i) surface resistivity ( $R_S$ ) and (ii) volume resistivity. The first measures the electrical conduction of materials with thickness  $H$  much less than width  $W$  and length  $L$ ; instead,  $R$  is the resistance and  $\rho$  the corresponding bulk resistivity of the sample. This quantity is given by  $R_S = R \times W/L = \rho/H$ . The measurement unit of surface resistivity in the International System is the Ohm ( $\Omega$ ). Besides, it is often used “Ohms per square” (indicated with  $\Omega/sq$ ), dimensionally equal to ohms, but used only for surface resistance to avoid misunderstandings. The volume resistivity is the current leakage resistance through the insulating material’s volumetric body, expressed in  $\text{ohm} \times \text{cm}^2$ . The higher volume resistivity means lower leakage current and, thus, lower conductance. Velostat has been recognized as one of the most stable, reliable, and therefore, probably the most promising polymeric composite material for the design of tactile sensors. The main advantages of this material are a flexible range of dimensions, mechanical and chemical stability, and relatively low price [16], [17]. All these specifications make the Velostat be developed from an alternative to traditional material in designing the force sensor. Among all previous fields, Velostat’s main field is the flexible sensor design, which has great implementations in robotics, wearable sensors, and human-machine interaction devices.

Ishita et al. [18], with Velostat, designed a wireless cumulative pressure measuring system. The LC circuit in the sensor is upgraded with LCR tank circuits using variable resistance from Velostat. The parameter such as input impedance, resonance frequency, and quality factors changes with the resistance change in Velostat/conductive foam on applying pressure. Yuan et al. [19], to effectively identify and detect an object, designed a pressure sensing system using Velostat. The designed system consists of an array of  $27 \times 27$  piezoresistive sensors using a Velostat and signal

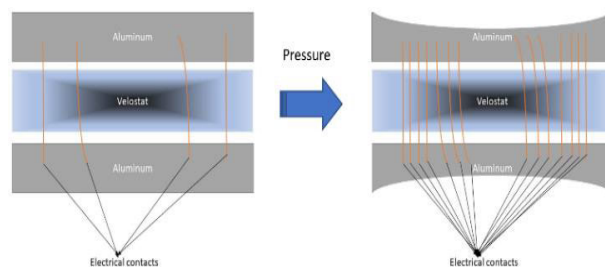


FIGURE 1. Velostat mechanism of pressure sensitive resistor.

processing module. For the classification of objects based on sensor array data, the convolutional neural network is employed. Accuracy of 98.54% was observed. Fatema et al. [20] designed a  $4 \times 4$  matrix shaped flexible pressure sensor using Velostat to measure the efficiency of patients performing physiotherapy. On the results obtained from the sensor system, neural networks are applied for effective position detection, and an error of 0.103 cm was detected, compared to the mathematical analysis error of 0.704 cm. Hopkins et al. [9] studied the implementation of sockets for use in lower limb prosthetic limbs using pressure sensitive Velostat. The designed system is implemented in real-time on one subject by verifying repeatability, accuracy, and hysteresis response. An average accuracy error of 110 kPa was observed, with a difference of 67% in the voltage. Hopkins et al. [21] developed a shoe for the detection of the gait phase with 174 independent sensing blocks using Velostat. The performance of the shoe is evaluated by asking the volunteer to walk in a straight line and turning. The mean absolute time of 45 ms to 58 ms and 51 ms to 77 ms for straight line and turning walking was observed between predicted phases and actual phase measurement.

This paper aims to develop a sensor sleeve that can be integrated into the fabric of any clothing article of choice by simple stitching, thereby maximizing flexibility. The novelty introduced in our paper is twofold: (i) we design both a smart sleeve using a force sensor made of Velostat and a novel resistive signal conditioning circuit (RSCC) to convert the change in the resistance of the sensor into an electric signal. The design of the smart sleeve is started with the development of a sensor patch. The design dimensions of the sensor patch is selected with the three preliminary tests conducted on Velostat to test the sensor properties: 1) dependence on the area of contact, 2) dependence on Velostat area, 3) dependence on the number of layers of Velostat. When a force is applied to the Velostat sensor (sensor patch), there is a change in resistance that is now converted to an electric signal using our novel RSCC. The signal from the RSCC is passed to the analog to digital converter (ADC) of the microcontroller, namely nRF51822, made by Nordic Semiconductors [22]. Finally, the data is transmitted to a smartphone through the Bluetooth low energy (BLE) module [23] present in the microcontroller. Then, (ii) we develop an Android app, by means of the

Android Studio integrated development environment (IDE), to process and utilize the sensor data. We design an application that can provide controls for the multimedia player of the smartphone. In the smart sleeve, we have four strips; hence, the pressure of each strip corresponds to a multimedia control (increase and/or decrease volume, play music, skip to the previous song, skip to the previous song). Moreover, music toggles pause/play when the third and fourth strips are pressed together. Finally, the pressure of all the strips simultaneously demonstrates the potential application of the system as an SOS alert system. By pressing all four sensing strips simultaneously, an SOS alert can be transmitted via the smartphone.

The remainder of the paper is organized as follows. The design process of the force sensor is started by conducting three preliminary tests on Velostat to study the properties, which are discussed in Section II-A. Then, the sensor patch is developed and discussed in Section II-B. The designing part of the RSCC is proposed in Section III. Further, the voltage from RSCC is applied as input to the microcontroller for analog to digital conversion. It transmits data wirelessly to a smartphone using BLE technology, which is discussed in Sections IV-A, IV-B, and IV-C, respectively. Results, discussion, and the Android Studio IDE used to develop applications for Android smartphones are discussed in Section V-A, V-B, and V-C respectively. Finally, our conclusions follow in Section VI.

## II. SENSOR TESTING AND PATCH DEVELOPMENT

### A. SENSOR PROPERTY TESTING

We need to design a sensor with maximum accuracy in measuring the input by ensuring suitable resistance to the sensor and acceptable change in resistance range when the force is applied. Velostat is suitable as it exhibits a volume resistivity of less than  $500 \Omega/cm$  [24], [19]. In recent years, Velostat has been used in applications like pressure sensing in the fields of soft robotics [9], robotic touch perception [25], robotic tactile interaction [26], and the hand strength distribution and gesture recognition [27]. Three preliminary tests are conducted on Velostat to test the sensor properties: 1) dependence on the area of contact, 2) dependence on Velostat area, 3) dependence on the number of layers of Velostat. The tests made use of square-shaped patches of Velostat and conductive cloth. Velostat patches are made of sizes  $4 \text{ cm}^2$ ,  $9 \text{ cm}^2$ ,  $16 \text{ cm}^2$ , and  $25 \text{ cm}^2$ , whereas conductive cloth patches are made of sizes  $1 \text{ cm}^2$ ,  $4 \text{ cm}^2$ ,  $9 \text{ cm}^2$ , and  $16 \text{ cm}^2$  respectively, as shown in Fig. 2(a). The results of the preliminary tests are presented in Section V. From the inferences drawn from the preliminary testing, we designed a sensor patch made of four individual strips of Velostat, each having four layers. Each strip of the sensor patch is connected to an RSCC.

### B. SENSOR PATCH DEVELOPMENT

Drawing insight from the tests performed in the previous section, a sensor array patch was designed. The

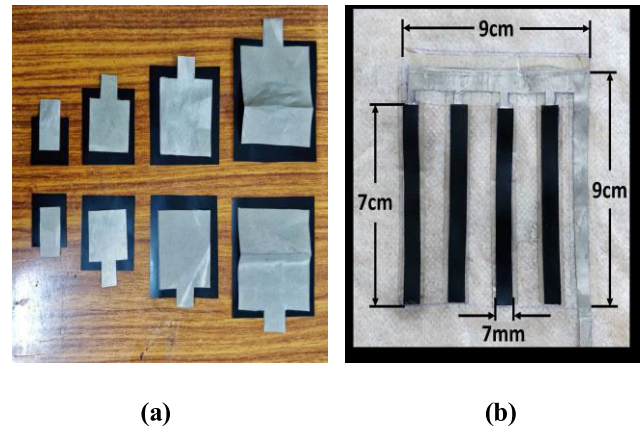


**FIGURE 2.** a) Sensor patches used for testing; b) Array of sensor paced in a 9cm x 9cm patch layout.

factors that are kept in mind when designing the patch were:

- small-sized patches provide a better range;
- more number of layers provides better range;
- smaller area of contact increases the resistance of every sensor.

The inferences drawn from the tests provide valuable groundwork for the design approach to follow. However, the physical limitations and constraints of the sensor patch are taken into account to ensure that it is practically implementable. Some limitations are:

- area of coverage;
- thickness;
- cost.

Thus, given the above constraints, tradeoffs, and parameters that influence the properties, the design of the patch is accurately performed. First, the overall size of the patch is determined to be 9 cm x 9 cm. The dimensions fall within the outer arm's limits and are also suitable for the forearm. For the layout of the sensing elements, four elements can provide a sufficient number of controls, not making the system overly complicated or power-consuming. To incorporate gestures like swipe, drag, and so on in the future, a simple parallel layout of the four elements, as longitudinal strips, is chosen. Next, the dimensions of each strip are selected. From the testing, we understand that a smaller Velostat strip has multiple benefits. Hence, to maintain a low net area while keeping the strips long enough to ensure a comfortable room for error, the individual strips are chosen to be of dimensions 7 cm X 7 mm, occupying a net area of only  $4.9 \text{ cm}^2$ . The low width also provides additional room between each sensing element (1.4 cm). The contact area can be minimized to keep the static resistance high and reduce the relatively expensive non-woven conductive cloth cost. Hence, longitudinal strips of 7 cm X 2 mm were chosen, with a total area of  $1.4 \text{ cm}^2$ , as shown in Fig. 2(b). Finally, each element is made to have four layers of Velostat to maximize the resistance range while keeping the thickness of the patch within limits to retain

flexibility. A simple comb-shaped common ground terminal is placed using non-woven conductive cloth connected to the bottom of all four sensing elements. The four strips of Velostat are then placed on top of each tooth of the comb structure, and the fifth segment is left free to become the ground terminal. The remaining three layers are placed on top of each strip. Subsequently, a single strip of non-woven conductive cloth is placed on top of each sensing element, which acts as the positive terminal for each sensing element.

### III. PROPOSED RESISTIVE SIGNAL CONDITIONING CIRCUIT

Being a piezoresistive material, Velostat senses the applied force by variation in its resistance and can be treated as a variable resistor. The variable resistor is placed in a voltage divider circuit, with a resistor in series, to find voltage change. The Velostat inside the sensor patch will generate resistance whenever there is a force applied on the sensor patch. The variable change in resistance from the sensor patch is provided to a novel RSCC to convert it into equivalent voltage. The operating voltage of the variable device is set to 3.3 V, as this is the voltage provided by common button cells such as CR2032 as well as one-cell Lipo batteries (3.7 V). So, 3.3 V will also act as a power supply for the voltage divider circuit. Since the patch we designed contains four strips of Velostat, four voltage divider circuits are connected in parallel.

On the designed patch, we observe a static zero force resistance of each strip to be approximately 5.2 k $\Omega$ , but when a user touch input is present, the minimum resistance observed is about 600  $\Omega$  to 1 k $\Omega$ . There is a variation between these two values based on the force applied to Velostat. We decided to use the minimum mean value of 800 $\Omega$  for the resistance of the Velostat patch in the presence of a user pressure. The ADC of the microcontroller nRF51822 has input voltage in the range of 0 to 1 V. So, we need to map resistance variation from 5.2 k $\Omega$  to 800  $\Omega$ , to 1 to 0 V. However, as it is impossible to observe 0 V across the Velostat (as the resistance will have to be 0  $\Omega$ ), it is mapped to 0.2 V instead. We know from voltage division that:

$$V_{out} = \frac{R_{vel}}{R_{vel} + R_{series}} \times 3.3V \quad (1)$$

Thus, mapping the zero force static resistance of  $R_{vel} = 5.2$  k $\Omega$  to  $V_{out} = 1$  V, we obtain resistance value  $R_{series} = 11.9$  k $\Omega$ . Similarly, mapping the applied force resistance of  $R_{vel} = 800$   $\Omega$  to  $V_{out} = 0.2$  V, we obtain  $R_{series} = 12.4$  k $\Omega$ . Thus, we use the mean value of resistance obtained for each case, which is 12 k $\Omega$ . The final schematic is shown in Fig. 3.

### IV. EMBEDDED SYSTEM DESIGN

#### A. HARDWARE

The system on a chip (SoC) used in this work is the nRF51822 by Nordic Semiconductors. It is an ultra-low power wireless transceiver SoC with BLE-4 support. The Velostat strips with

the proposed RSCC are connected as direct analog inputs to the ADC channels of the nRF51822 microcontroller. The values can then be read in real-time using the application code. The voltage applied across the whole circuit is 3.3V. The other hardware aspect of this system is the smartphone which receives the sensor data sent by the microcontroller. The phone needs BLE transceiving hardware and software support through the operating system.

#### B. SOFTWARE

The software protocol stack called the BLE SoftDevice made by Nordic Semiconductors runs on the nRF51822 microcontroller, implementing core BLE functions and interacting with the application code. The application code written by the user resides over the SoftDevice and implements the microcontroller-specific functionality along with setting up the BLE attributes and Interrupt Service Routines. The online compiler and IDE called Mbed by ARM [28] were used to write and compile the application code. The resultant binary firmware file is uploaded into the nRF51822 microcontroller. Fig. 4 presents the flowchart of the embedded code uploaded on the nRF51822 microcontroller, while Algorithm 1 shows the pseudo-code of the same algorithm. The BLE API of the Android operating system is used in developing the mobile application for Android smartphones. The app uses Android Studio IDE [29] and Java programming language.

---

#### Algorithm 1 Algorithm of Pseudo-Code For nRF51822 Microcontroller

---

**Input:** Sensor data from velostat strips

**Output:** Updated BLE characteristics

- 1: Declare four analog pins connected to velostat strips
  - 2: Initialize ADC
  - 3: Define BLE parameters
  - 4: Initialize timer for 10 ms and assign to *periodcallback()*
  - 5: Initialize BLE and advertise with defined parameters
  - 6: Add a new service, "Sensor Value Service"
  - 7: Add "Sensor Value Characteristic" under "Sensor Value Service" with an array of four floating point variables concerning to the four velostat strips
  - 8: **while** (1) **do**
  - 9:     **if** (Sensor polling == TRUE) **then**
  - 10:         Read values from ADC corresponding to the sensor strip's data
  - 11:         Upload BLE characteristics with data received from sensor
  - 12:         Switch OFF sensor polling
  - 13:     **Else**
  - 14:         Wait for BLE events (till the sensor strip data is updated)
  - 15:         ON power saving mode
  - 16:     **end if**
  - 17: **end while**
-



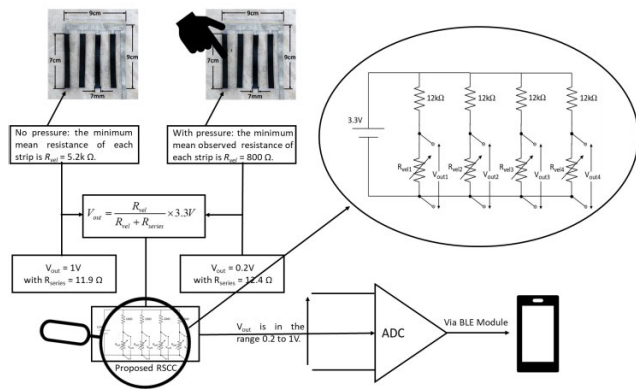


**FIGURE 3.** Diagram of the whole proposed system, from the Velostat sensitive resistor to the Android app on the smartphone via BLE module, plus the novel RSCC.

**C. BLE**

Any BLE-enabled device can be categorized as a peripheral or a central in the generic access profile (GAP) level. GAP deals with basic lower-level BLE network attributes and sets up the device as a broadcaster or observer. In our case, the nRF51822 acts as the peripheral, broadcasting its presence with nearby central devices. The device categorization is client and server on the higher level called generic attribute profile (GATT). GATT deals with how the devices handle and exchange the actual data to be sent or received. In this case, the nRF51822 sends sensor data to the connected (at GAP level) and listens to client devices, so it is a BLE GATT server. The low-level connection attributes handled by GAP are important factors in determining the data rate and latency between two connected devices. The advertisement attributes include device name, service universally unique identifiers (UUID), extra advertisement payload, advertisement type, and the advertising interval. Other attributes are connection attributes, connection interval (the amount of time after which the device can transfer data again, the least value of 7.5 ms is being used), slave latency (number of requests which can be ignored if there is no new data to send) and connection supervision timeout (amount of time to wait before declaring a connection as lost if no data transfers took place, currently 6 seconds).

The GATT server creates a GATT service and GATT characteristic, each with a different UUID that defines the application for which the GATT profile is used. Each device can exhibit many services. Each service can have many characteristics, each of which will send different data related to the service. In our application, we create a service called Sensor service and a characteristic under it called Sensor Value Characteristic and assign UUID to them.

**V. RESULTS AND DISCUSSION**

**A. PRELIMINARY TESTS ON SENSOR MATERIAL**

For the first preliminary test, namely test 1, a fixed area of Velostat (25 cm<sup>2</sup>) is subjected to three different weights (50 g,

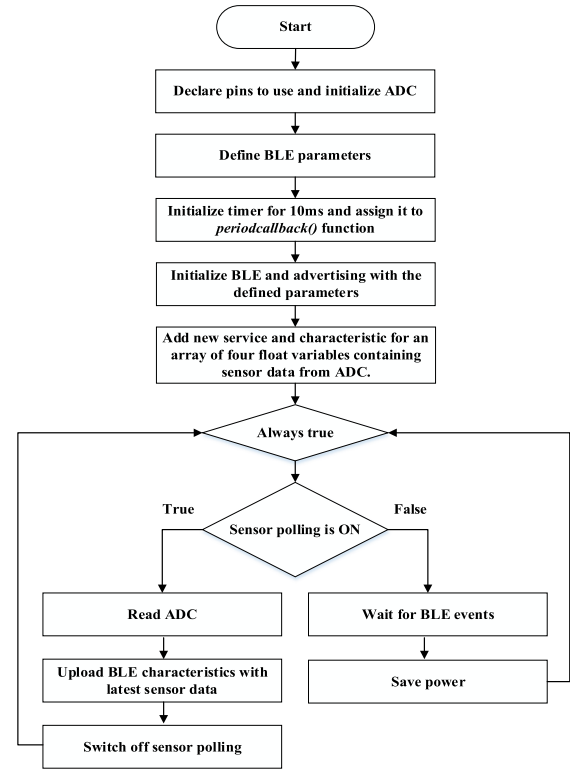


**FIGURE 4.** Flowchart of the nRF51822 embedded code.

100 g, and 150 g), with four different areas of contacts (1 cm<sup>2</sup>, 4 cm<sup>2</sup>, 9 cm<sup>2</sup>, and 16 cm<sup>2</sup>). The results of the test 1 are shown in Fig. 5. It is a plot of resistance versus the area of contact fixing the area of Velostat constant at 25 cm<sup>2</sup>. The test showed a proportional decreasing in resistance with an increasing in the area of contact. However, the range of resistance change remains constant over the change in the contact area.

For the second preliminary test, namely test 2, a fixed area of contact (1 cm<sup>2</sup>) is subjected to three different weights (50 g, 100 g, and 150 g), with four different areas of Velostat (4 cm<sup>2</sup>, 9 cm<sup>2</sup>, 16 cm<sup>2</sup>, and 25 cm<sup>2</sup>). Fig. 6 shows the results of the test 2. It is a plot of resistance versus the area of Velostat, fixing the area of contact constant at 1 cm<sup>2</sup>. Here we observe again that the resistance decreases with an increasing in the area of Velostat.

However, we also notice that the change in resistance for a fixed change in weight is greater at low areas and decreases as the area of Velostat increases. Hence, we can obtain a greater range of values for a change in force when the area of Velostat is low, thereby providing better accuracy.

In the final preliminary test, namely test 3, the fixed area of Velostat (25 cm<sup>2</sup>) and area of contact (1 cm<sup>2</sup>) are subjected to 5 layers of Velostat. Fig. 7 shows the results of the test 3. It is a plot of resistance versus the number of layers of Velostat fixing the area of Velostat and the area of contact constant at 25 cm<sup>2</sup> and 1 cm<sup>2</sup>. From the figure, we can see how an increasing in layers produces a significant increasing in resistance.

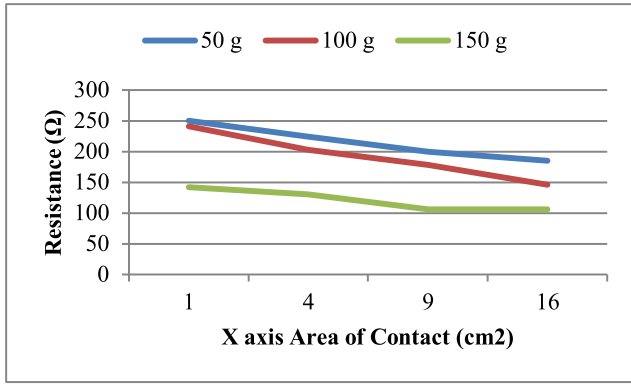


FIGURE 5. Plot of resistance vs area of contact for a fixed area of Velostat

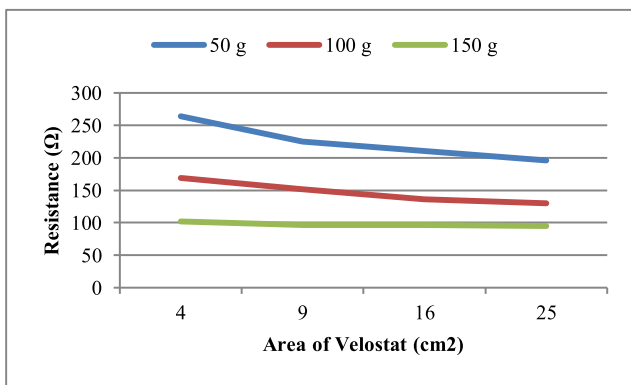


FIGURE 6. Plot of resistance vs area of Velostat for a fixed area of contact.

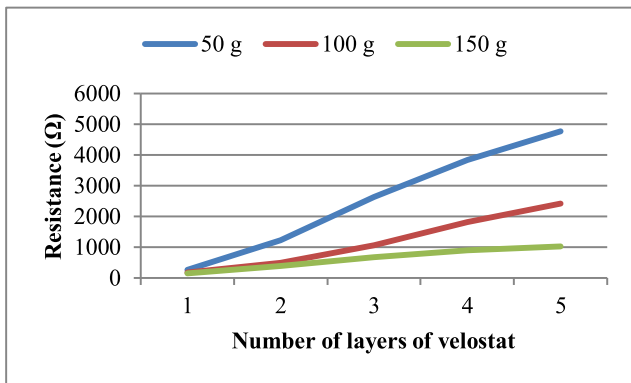


FIGURE 7. Plot of resistance vs number of layers of Velostat for a fixed area of contact and Velostat size.

**B. MEASUREMENT SET-UP**

The initial measurement setup ie. sensor patch and RSCC is presented in Fig. 8. After designing the optimum sensor patch, the novel RSCC that converts the change in the resistance of the sensor into an electric signal and the Android app, we now need to check if the real-time human pressure of each strip corresponds to a multimedia control in the Android app (e.g., increase and/or decrease volume, play music, skip to the previous song, skip to the previous song).

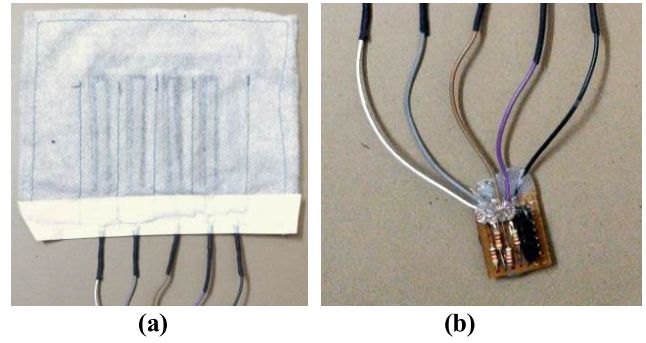


FIGURE 8. Snapshot of (a) sensor patch (b) resistive signal conditioning circuit (RSCC).

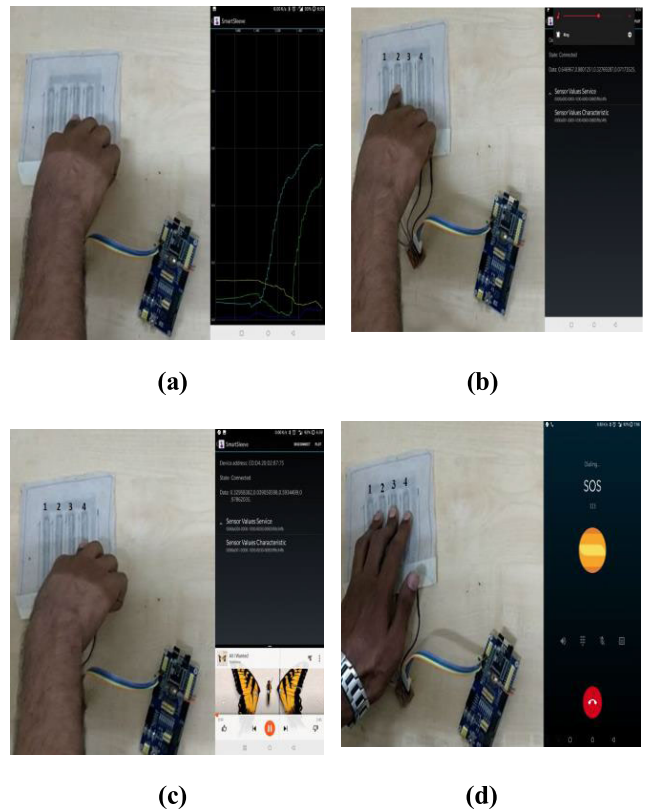


FIGURE 9. Measurement set-up: a) real-time plotting of sensor values; b) real-time volume increasing/decreasing; c) real-time playback multimedia control; d) real-time SOS alert activating.

Fig. 9(a) presents the raw analog values of the sensor as plotted by the application. Each sensing strip is allotted a color, as can be seen. The green color represents the third strip; hence, the green line rises when the third strip is pressed. Fig. 9(b) shows what happens when the human pressure is applied to the first or second strip (i.e., volume decrease or increase on a smartphone playing music). The first and second strips are in fact assigned to these functions; hence, the volume can be seen to reduce (increase) on the real-time pressing of the second (first) strip. Fig. 9(c) demonstrates how the real-time pressure of the third or fourth

**TABLE 1.** Strip functionality.

Strip	Task
Only 1st strip volume increase	Only 1st strip volume increase
Only 2nd strip volume decrease	Only 2nd strip volume decrease
Only 3rd strip previous song	Only 3rd strip previous song
Only 4th strip next song	Only 4th strip next song
1st, 2nd, 3rd and 4th strips SOS alert	1st, 2nd, 3rd and 4th strips SOS alert

---

**Algorithm 2** Algorithm for Implementation of Android Application
 

---

- 1: Power up the wireless smart sleeve device
  - 2: In the mobile phone, turn on the Bluetooth
  - 3: Open Smart Sleeve android application
  - 4: Search for Bluetooth devices and select wireless smart sleeve device
  - 5: The confirmation of connection is visible in the “state” option as “connected” in the Android application
  - 6: On the Android application, select the visible service “Sensor Value Service”
  - 7: Select “Sensor Value Characteristic,” available below “Sensor Value Service”
  - 8: Now the Android application starts receiving data from wireless smart sleeve device and is visible in the option “Data” with four values
  - 9: **while** (1) **do**
  - 10:   Select whether sensor values need to be plotted or implement functionality
  - 11:   **if** (Plot sensor values) **then**
  - 12:     Select plot option
  - 13:     A plot window is opened
  - 14:     Upon pressing any strip on the wireless smart sleeve device concerned signal goes high
  - 15:   **else if** (Implement functionality) **then**
  - 16:     Upon pressing any strip on the wireless smart sleeve device designated task listed across the strip in Table 1 is performed concerned the signal goes high
  - 17:   **end if**
  - 18: **end while**
- 

strip can activate the music playback control on a smartphone. The third and fourth strips are assigned to these functions; hence, the music can change to the previous (next) song pressing the third (fourth) strip. Moreover, music toggles pause/play when the third and fourth strips are pressed together.

Fig. 9(d) demonstrates the real-time potential application of the system as an SOS alert system. By pressing all four sensing strips simultaneously, as shown, an SOS alert can be transmitted via the smartphone. Table 1 presents the summary of the task allocated against each strip.

### C. ANDRIOD APPLICATION

We designed our application relying on the main principles of software analysis and design. In particular, we exploit the Layer and Model View Presenter (MVP) design patterns. The reason for using the MVP pattern is that it allows us to separate software responsibilities across three main components: (i) the Model component groups the data that should be displayed in the User Interface (UI); (ii) the View component renders the User Interface (UI) elements; (iii) the Presenter component manages the interaction between the UI and the application logic by retrieving and formatting the data that should be displayed to end-users. The application we design runs on the Android operating system on any smartphone.

The six steps performed by the application are:

- 1) Scanning for BLE devices and connecting to them.
- 2) Distinguishing between smart sleeve and other BLE devices using GATT UUID.
- 3) Real-time plotting of four channels of sensor data.
- 4) Smoothing the sensor data using a primitive Lowpass filter.
- 5) Music playback control using sensor data.
- 6) Signal of Stress (SOS) functionality using sensor data.

In Algorithm 2, the pseudo-code for the implementation of the Android Application algorithm is illustrated.

### VI. CONCLUSION AND FUTURE SCOPE

In this paper, we have designed a wireless smart sleeve built on the Velostat sensitive pressure sensor. The smart sleeve is connected to a smartphone, and based on the touch provided on the sleeve, the assigned task gets executed on the smartphone. We have first carried out three preliminary tests to design the optimum sensor patch. Then, we have designed a novel resistive signal conditioning circuit to connect this sensor patch to the microcontroller nRF51822. The BLE module in the microcontroller transmits data to the Android Studio IDE application developed for Android smartphones. The smart sleeve we have proposed is a fully functional wearable device in portable consumer electronics. The device is a useful daily accessory that is cost-effective, keeps the user free of distractions while driving, and can help in emergencies. The sensor may falsely trigger the application by accident, but this can be minimized when conductive threads are used, as the object must be conductive for the sensor to pick up any signal. Further work can be done to make the system responsive to more complicated forms of inputs, such as gestures. Gestures (e.g., swiping) allow for a deeper, more versatile control. This can be done by improvising the signals’ processing using artificial neural networks.

### REFERENCES

- [1] X. Song, M. Wang, H. Qiu, K. Li, and C. Ang, “Auditory scene analysis-based feature extraction for indoor subarea localization using smartphones,” *IEEE Sensors J.*, vol. 19, no. 15, pp. 6309–6316, Aug. 2019.
- [2] V. Annepu, D. R. Sona, C. V. Ravikumar, K. Bagadi, M. Alibakhshikenari, A. A. Althuwayb, B. Alali, B. S. Virdee, G. Pau, I. Dayoub, C. H. See, and F. Falcone, “Review on unmanned aerial vehicle assisted sensor node localization in wireless networks: Soft computing approaches,” *IEEE Access*, vol. 10, pp. 132875–132894, 2022.



- [3] V. Annepu, A. Rajesh, and K. Bagadi, "Radial basis function-based node localization for unmanned aerial vehicle-assisted 5G wireless sensor networks," *Neural Comput. Appl.*, vol. 33, no. 19, pp. 12333–12346, Oct. 2021.
- [4] A. Amjad, M. Patwary, A. Griffiths, and A.-H. Soliman, "Characterization of field-of-view for energy efficient application-aware visual sensor networks," *IEEE Sensors J.*, vol. 16, no. 9, pp. 3109–3122, May 2016.
- [5] L. Huang, J. Chen, Y. Xu, D. Hu, X. Cui, D. Shi, and Y. Zhu, "Three-dimensional light-weight piezoresistive sensors based on conductive polyurethane sponges coated with hybrid CNT/CB nanoparticles," *Appl. Surf. Sci.*, vol. 548, May 2021, Art. no. 149268. [Online]. Available: <https://www.sciencedirect.com/science/article/pii/S0169433221003445>
- [6] Y. Xiong, Y. Shen, L. Tian, Y. Hu, P. Zhu, R. Sun, and C.-P. Wong, "A flexible, ultra-highly sensitive and stable capacitive pressure sensor with convex microarrays for motion and health monitoring," *Nano Energy*, vol. 70, Apr. 2020, Art. no. 104436. [Online]. Available: <https://www.sciencedirect.com/science/article/pii/S221128551931153X>
- [7] S. Wang, H.-Q. Shao, Y. Liu, C.-Y. Tang, X. Zhao, K. Ke, R.-Y. Bao, M.-B. Yang, and W. Yang, "Boosting piezoelectric response of PVDF-TrFE via MXene for self-powered linear pressure sensor," *Compos. Sci. Technol.*, vol. 202, Jan. 2021, Art. no. 108600. [Online]. Available: <https://www.sciencedirect.com/science/article/pii/S0266353820323915>
- [8] G. Yao, L. Xu, X. Cheng, Y. Li, X. Huang, W. Guo, S. Liu, Z. L. Wang, and H. Wu, "Bioinspired triboelectric nanogenerators as self-powered electronic skin for robotic tactile sensing," *Adv. Funct. Mater.*, vol. 30, no. 6, Feb. 2020, Art. no. 1907312, doi: [10.1002/adfm.201907312](https://doi.org/10.1002/adfm.201907312).
- [9] M. Hopkins, R. Vaidyanathan, and A. H. McGregor, "Examination of the performance characteristics of Velostat as an in-socket pressure sensor," *IEEE Sensors J.*, vol. 20, no. 13, pp. 6992–7000, Jul. 2020.
- [10] X. Chen, D. Zhang, H. Luan, C. Yang, W. Yan, and W. Liu, "Flexible pressure sensors based on molybdenum disulfide/hydroxyethyl cellulose/polyurethane sponge for motion detection and speech recognition using machine learning," *ACS Appl. Mater. Interface*, vol. 15, no. 1, pp. 2043–2053, Jan. 2023, doi: [10.1021/acami.2c16730](https://doi.org/10.1021/acami.2c16730).
- [11] H. Zhang, D. Zhang, B. Zhang, D. Wang, and M. Tang, "Wearable pressure sensor array with layer-by-layer assembled MXene nanosheets/Ag nanoflowers for motion monitoring and human-machine interfaces," *ACS Appl. Mater. Interface*, vol. 14, no. 43, pp. 48907–48916, Nov. 2022, doi: [10.1021/acami.2c14863](https://doi.org/10.1021/acami.2c14863).
- [12] H. Xia, D. Zhang, D. Wang, M. Tang, H. Zhang, X. Chen, R. Mao, Y. Ma, and H. Cai, "High sensitivity, wide range pressure sensor based on layer-by-layer self-assembled MXene/carbon Black@Polyurethane sponge for human motion monitoring and intelligent vehicle control," *IEEE Sensors J.*, vol. 22, no. 22, pp. 21561–21568, Nov. 2022.
- [13] W. Zhao, D. Zhang, Y. Yang, C. Du, and B. Zhang, "A fast self-healing multifunctional polyvinyl alcohol nano-organic composite hydrogel as a building block for highly sensitive strain/pressure sensors," *J. Mater. Chem. A*, vol. 9, no. 38, pp. 22082–22094, 2021, doi: [10.1039/d1ta05586k](https://doi.org/10.1039/d1ta05586k).
- [14] *3 MTM Electronics Materials Solutions Division 3MTM Conductive Film Products*. [Online]. Available: <http://documents.staticcontrol.com/pdf/2004.pdf>
- [15] R. de Fazio, E. Perrone, R. Velázquez, M. De Vittorio, and P. Visconti, "Development of a self-powered piezo-resistive smart insole equipped with low-power BLE connectivity for remote gait monitoring," *Sensors*, vol. 21, no. 13, p. 4539, 2021. [Online]. Available: <https://www.mdpi.com/1424-8220/21/13/4539>
- [16] D. Giovanelli and E. Farella, "Force sensing resistor and evaluation of technology for wearable body pressure sensing," *J. Sensors*, vol. 2016, pp. 1–13, Sep. 2016.
- [17] J. Ahmad, H. Andersson, and J. Sidén, "Screen-printed piezoresistive sensors for monitoring pressure distribution in wheelchair," *IEEE Sensors J.*, vol. 19, no. 6, pp. 2055–2063, Mar. 2019.
- [18] I. Bhar and N. Mandal, "Design of a wireless passive pressure measurement system using piezoresistive materials," *IEEE Sensors J.*, vol. 22, no. 22, pp. 21518–21526, Nov. 2022.
- [19] L. Yuan, H. Qu, and J. Li, "Velostat sensor array for object recognition," *IEEE Sensors J.*, vol. 22, no. 2, pp. 1692–1704, Jan. 2022.
- [20] A. Fatema, S. Poondla, R. B. Mishra, and A. M. Hussain, "A low-cost pressure sensor matrix for activity monitoring in stroke patients using artificial intelligence," *IEEE Sensors J.*, vol. 21, no. 7, pp. 9546–9552, Apr. 2021.
- [21] X. Hu, Q. Duan, J. Tang, G. Chen, Z. Zhao, Z. Sun, C. Chen, and X. Qu, "A low-cost instrumented shoe system for gait phase detection based on foot plantar pressure data," *IEEE J. Transl. Eng. Health Med.*, early access, Sep. 26, 2023, doi: [10.1109/JTEHM.2023.3319576](https://doi.org/10.1109/JTEHM.2023.3319576).
- [22] *Multiprotocol Bluetooth Low Energy/2.4 GHz RF System on Chip*, Nordic Semiconductor, document nRF51822, 2014.
- [23] Y. Yu, R. Chen, L. Chen, X. Zheng, D. Wu, W. Li, and Y. Wu, "A novel 3-D indoor localization algorithm based on BLE and multiple sensors," *IEEE Internet Things J.*, vol. 8, no. 11, pp. 9359–9372, Jun. 2021.
- [24] B. W. Lee and H. Shin, "Feasibility study of sitting posture monitoring based on piezoresistive conductive film-based flexible force sensor," *IEEE Sensors J.*, vol. 16, no. 1, pp. 15–16, Jan. 2016.
- [25] G. Pugach, A. Melnyk, O. Tolochko, A. Pitti, and P. Gausser, "Touch-based admittance control of a robotic arm using neural learning of an artificial skin," in *Proc. IEEE/RSI Int. Conf. Intell. Robots Syst. (IROS)*, Oct. 2016, pp. 3374–3380.
- [26] A. Dzedzickis, E. Sutynis, V. Bucinskas, U. Samukaite-Bubniene, B. Jakstys, A. Ramanavicius, and I. Morkvenaite-Vilkonciene, "Polyethylenecarbon composite (Velostat®) based tactile sensor," *Polymers*, vol. 12, no. 12, p. 2905, 2020. [Online]. Available: <https://www.mdpi.com/2073-4360/12/12/2905>
- [27] C. Mummadi, F. Leo, K. Verma, S. Kasireddy, P. Scholl, J. Kempfle, and K. Laerhoven, "Real-time and embedded detection of hand gestures with an IMU-based glove," *Informatics*, vol. 5, no. 2, p. 28, Jun. 2018. [Online]. Available: <https://www.mdpi.com/2227-9709/5/2/28>
- [28] *Mbed*. Accessed: Aug. 10, 2023. [Online]. Available: <https://ide.mbed.com/compiler/>
- [29] *Download Android Studio and SDK Tools: Android Developers*. Accessed: Aug. 10, 2023. [Online]. Available: <https://developer.android.com/studio>



**KRANTHI KUMAR PULLURI** received the B.Tech. degree in electronics and communication engineering from Jawaharlal Nehru Technological University, Hyderabad, India, in 2008, and the M.Tech. degree in automotive electronics from the Vellore Institute of Technology, Vellore, India, in 2010, where he is currently pursuing the Ph.D. degree in electronics and communication engineering. He has published one paper in IEEE SENSORS JOURNAL and one paper IEEE conferences.

His research interests include sensors and signal conditioning, electronic nose, machine learning, and embedded systems.



**VAEGAE NAVEEN KUMAR** (Senior Member, IEEE) received the B.Tech. degree in instrumentation engineering from Nagarjuna University, Guntur, India, in 2001, the M.Tech. degree in electronics engineering from Jawaharlal Nehru Technological University, Kakinada, India, in 2010, and the Ph.D. degree in electrical and electronics engineering from the Vellore Institute of Technology, Vellore, India. He is currently an Associate Professor with the School of Electronics Engineering,

Vellore Institute of Technology. He has authored over 15 SCIEF publications and over 16 Scopus indexed journals and conferences. His publications are in IEEE SENSORS JOURNAL, *Biocybernetics and Biomedical Engineering*, *Biomedical Signal Processing and Control*, *Sensors and Actuators A: Physical*, *Measurement: Journal of the International Measurement Confederation*, and *IET Science Measurement & Technology*. His research interests include sensors and signal conditioning, signal processing, soft computing, intelligent systems, electronic nose, genomic signal processing, and the IoT. He is a lifetime member of ISTE and a member of International Association of Engineering. He has been a Faculty Advisor and a Coordinator of IEEE Signal Processing Society, VIT Student Chapter, since 2017.





**KALAPRAVEEN BAGADI** (Member, IEEE) received the B.E. degree in electronics and communication engineering from Andhra University, India, in 2006, and the M.Tech. degree in electronic systems and communication and the Ph.D. degree in wireless communication from the Department of Electrical Engineering, National Institute of Technology, Rourkela, India, in 2009 and 2014, respectively. He was a Full Professor with the School of Electronics Engineering (SENSE), Vellore Institute of Technology (VIT), Vellore, India, until April 2023. Currently, he is with the School of Electronics Engineering (SENSE), VIT-AP University, Amaravati, Andhra Pradesh, India. His research interests include SDMA, MIMO, OFDM, NOMA, D2D communication, cognitive radio, UAV communication, and artificial intelligence. He has completed six Ph.D. theses under his guidance and is currently guiding three scholars. He is an Academic Editor of *Wireless Communication and Mobile Computing* and *Applied Computational Intelligence and Soft Computing*. He also reviews journals like IEEE ACCESS, *Wireless Personal Communications*, *IET Communications*, and *Telecommunication Systems*. He has published over 50 research articles in various refereed international journals, such as IEEE ACCESS, *Neural Computing and Applications*, *Wireless Personal Communication*, *IET Communication*, *International Journal of Communication Systems*, and *Radio Science*. His work has been cited over 600 times on Google Scholar with an H-index of 13.



**VISALAKSHI ANNEPU** received the B.Tech. degree in computer science and engineering from Jawaharlal Nehru Technical University, Kakinada, India, in 2011, the M.Tech. degree in computer science and Technology from Andhra University, Visakhapatnam, India, in 2013, and Ph.D. degree in computer networks from VIT Vellore, India, in 2020. She was an Assistant Professor with the Department of Computer Engineering, Sri Sivani Institute of Technology, Srikakulam, Andhra Pradesh, from June 2014 to May 2016. Currently, she is an Assistant Professor with the School of Computer Science and Engineering, VIT-AP University, Amaravati, India. Her research interests include wireless networking, artificial intelligence, soft computing techniques, and neural networks.



**FRANCESCO BENEDETTO** (Senior Member, IEEE) has been the Chair of the IEEE 1900.1 standard “Definitions and Concepts for Dynamic Spectrum Access: Terminology Relating to Emerging Wireless Networks, System Functionality, and Spectrum Management,” since 2016. He has been the Leader of the WP 3.5 on “Development of Advanced GPR Data Processing Technique” of the European COST Action TU1208-Civil Engineering Applications of Ground Penetrating Radar. He is currently an Associate Editor of IEEE ACCESS, an Editor of the IEEE SDN Newsletter, an Associate Editor of the *AEÜ—International Journal of Electronics and Communications* (Elsevier), the Editor-in-Chief of the international journal *Recent Advances on Computer Science and Communications* (Bentham), the General Co-Chair of the IEEE 43rd International Conference on Telecommunications and Signal Processing (TSP 2020), the General Chair of the Series of International Workshops on Signal Processing for Secure Communications (SP4SC 2014, 2015, and 2016), and the Lead Guest Editor of the Special Issue on “Advanced Ground Penetrating Radar Signal Processing Techniques” of the *Signal Processing Journal* (Elsevier). He also served as a reviewer and a TPC member for several IEEE international conferences and symposia for several IEEE TRANSACTIONS, IET Conference Proceedings, EURASIP, and Elsevier journals.

...